Physica D 31 (1988) 190–211
North-Holland, Amsterdam

CHAOTIC DYNAMICS OF A WHIRLING PENDULUM*

Steven W. SHAW
Department of Mechanical Engineering, Michigan State University, East Lansing, MI 48824, USA

and

Stephen WIGGINS
Applied Mechanics, California Institute of Technology, Pasadena, CA 91125, USA

Received 24 February 1987
Revised manuscript received 25 January 1988
Communicated by J.E. Marsden

A physical system is considered consisting of a rigid frame which is free to rotate about a vertical axis and to which is attached a planar simple pendulum. This system has "one and a half" degrees of freedom due to the fact that the frame and pendulum may freely rotate about the vertical axis, i.e., conservation of angular momentum holds for the "ideal," or unperturbed, system. Using a Hamiltonian formulation we reduce the unperturbed equations of motion to a conservative planar system in which the constant angular momentum plays the role of a parameter. This system is shown to possess one or two sets of homoclinic motions depending on the level of the angular momentum. When this system is perturbed by external excitations and dissipative forces these homoclinic motions can break into homoclinic tangles providing the conditions for chaotic motions of the horseshoe type to exist. The criteria for this to occur can be formulated using a variation of Melnikov's method developed for slowly varying oscillators [1, 2]. For the present problem, the angular momentum becomes a slowly varying parameter upon addition of the disturbances. These ideas are used to rigorously prove the existence of chaotic motions for this system and to compute, to first order, global bifurcation parameter conditions. Since two types of homoclinic motions can occur, two different chaotic modes of motion can result and physical interpretations of these motions are given. In addition, a limiting case is considered in which the system becomes a single degree of freedom oscillator with parametric excitation.

1. Introduction

There now exist many examples of single degree of freedom nonlinear oscillators which exhibit chaotic motions when subjected to periodic excitation; see, for example, [3–7]. These motions typically arise due to the transversal intersection of stable and unstable manifolds of a saddle type periodic motion, thus resulting in the Smale horseshoe type of chaos [9].

If one starts with a conservative planar system, i.e., a conservative single degree of freedom oscillator, with multiple equilibria, often the saddle points separating the stable equilibria are connected to themselves via a saddle-loop, or homoclinic trajectory; i.e., the stable and unstable manifolds coincide. Such trajectories form the mechanism for certain types of chaotic motions. Using Melnikov's method one can compute conditions on the parameters for which these transverse intersections, and hence chaos, can occur. The method does not guarantee the existence of a strange attractor, i.e., steady state chaos, but does give a bound in parameter space below which chaos is unlikely to occur. This has been verified experimentally for some systems [5, 7].

*Supported in part by NSF Grant 86-13294 and by DARPA.

0167-2789/88/$03.50 © Elsevier Science Publishers B.V.

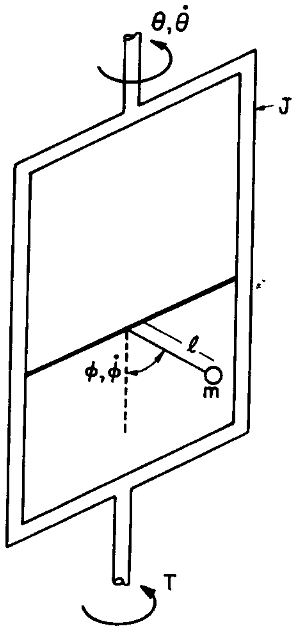

Fig. 1. The whirling pendulum. Mass m is restricted to a plane perpendicular to the frame J.

The system to be considered here is depicted in fig. 1. It consists of a rigid frame which freely rotates about a vertical axis and to which a planar pendulum is attached, the pivot being on the vertical axis. The behavior of this system is well known if the frame rotation rate, $\dot{\theta}$, is held at a constant value, say Ω. Below a critical Ω the pendulum behaves essentially like a nonrotating pendulum, it has a stable equilibrium at $\phi = 0$ and an unstable one at $\phi = \pi$. Above the critical Ω value, $\phi = 0$ becomes unstable and two new equilibria appear at $\phi = \bar{\phi} = \pm\cos^{-1}[(g/l)/\Omega^2]$. As $\Omega \to \infty$, $\bar{\phi} \to \pm\pi/2$ as expected.

If one were to add small dissipation at the pendulum pivot and allow a small periodic variation in $\dot{\theta}$, i.e., set $\dot{\theta} = \bar{\Omega} + \varepsilon\tilde{\Omega}\cos(\omega t)$ $(0 < \varepsilon \ll 1)$, the system becomes a forced oscillator similar to those found in refs. [3–7] and the usual Melnikov analysis can be used to predict the onset of chaotic motions. This type of perturbation is considered below as a limiting case of our more general system in which $\dot{\theta}$ is allowed to vary in accordance with the equation which governs the behavior of the angular momentum of the system.

The system considered here has "one and a half" degrees of freedom. The rotation of the frame is coupled to the motion of the pendulum via an angular momentum relationship. The orientation of the frame, measured by the variable θ, does not appear in the unperturbed equations of motion. In a Hamiltonian formulation one immediately obtains two constants of motion in the unperturbed case: the energy and the conjugate momentum associated with θ, hence this system is completely integrable. Upon the addition of small perturbations, the angular momentum and energy will vary slowly in time and this variation affects the occurrence of chaotic motions. The results in this paper should be of interest to experimentalists since often in rotating systems one can specify the applied torques but not necessarily the rotation speed itself.

It is interesting to note that this rotating pendulum is very similar to the flyball governer which is used for speed control. Among its many uses, it was employed by the astronomer-mathematician G.B. Airy in the mid 1800's for observing fixed stars for extended periods by moving a telescope in opposition to the earth's rotation. He observed that the device was not always stable: "...and the machine (if I may so express myself) became perfectly wild" (Airy [8]). Of course it is not known whether or not the motion Airy observed was chaotic, but we show in the following that chaos can occur in a similar mechanism.

This paper is arranged as follows. Section 2 describes the equations of motion and the structure of the phase space for both the unperturbed and the perturbed systems where the perturbations are considered to be periodic in time. The subsequent section describes the application of Melnikov's method to the problem and describes the nature of the chaotic motions which can result. Section 4 describes a limiting case in which the system becomes an ordinary parametrically excited single degree of freedom oscillator; a Melnikov analysis is given for this case also. Perturbations which are periodic in the rotational variable θ are considered in section 5. Again, Melnikov's method for this situation is given and the results are compared with those for time periodic excitation. The paper is closed with a summary and a few remarks in section 6.

2. Equations of motion and the structure of the phase space

2.1. *The unperturbed system*

Referring to fig. 1 one can write the nondimensionalized kinetic and potential energies as

$$T(\phi, \dot{\phi}, \dot{\theta}) = \frac{\hat{T}}{mgl} = \tfrac{1}{2}(\mu + \sin^2\phi)\dot{\theta}^2 + \tfrac{1}{2}\dot{\phi}^2, \tag{2.1}$$

$$V(\phi) = \frac{\hat{V}}{mgl} = 1 - \cos\phi, \tag{2.2}$$

where the quantities with circumflexes are unscaled, time has been rescaled by the nonrotating pendulum frequency, $t = \sqrt{(g/l)}\,\tau$, and $(\dot{\ }) = \mathrm{d}/\mathrm{d}t$ represents a derivative with respect to the dimensionless time t. The parameter μ is a measure of the ratio of the frame rotational inertia J to the pendulum inertia, ml^2, i.e., $\mu = J/ml^2$.

The analysis in this paper is most easily done if a first order, Hamiltonian approach is employed. Hence, the conjugate momenta for the system are defined as

$$p_\phi = \frac{\partial T}{\partial \dot{\phi}} = \dot{\phi}, \tag{2.3}$$

$$p_\theta = \frac{\partial T}{\partial \dot{\theta}} = (\mu + \sin^2\phi)\dot{\theta}, \tag{2.4}$$

and the kinetic energy can be written in terms of these as

$$T(\phi, p_\phi, p_\theta) = \tfrac{1}{2}\left(p_\theta^2/(\mu + \sin^2\phi)\right) + \tfrac{1}{2}p_\phi^2. \tag{2.5}$$

The Hamiltonian is time-independent and is easily formed as follows:

$$H(\phi, p_\phi, p_\theta) = T(\phi, p_\phi, p_\theta) + V(\phi), \tag{2.6}$$

and provides, via Hamilton's equations, the unperturbed equations of motion

$$\dot{\phi} = \frac{\partial H}{\partial p_\phi} = p_\phi, \tag{2.7a}$$

$$\dot{p}_\phi = \frac{\partial H}{\partial \phi} = \sin\phi\left(-1 + p_\theta^2 \cos\phi/\left(\mu + \sin^2\phi\right)^2\right), \tag{2.7b}$$

$$\dot{\theta} = \frac{\partial H}{\partial p_\theta} = \frac{p_\theta}{\mu + \sin^2\phi}, \tag{2.7c}$$

$$\dot{p}_\theta = \frac{\partial H}{\partial \theta} = 0. \tag{2.7d}$$

Eq. (2.7d) is simply a statement of conservation of angular momentum and eq. (2.7c) uncouples from the other equations since θ appears nowhere on the right-hand side. These observations allow a reduction of the system to a single degree of freedom conservative oscillator in the variables ϕ and p_ϕ, with equations of motion (2.7a, b) which depend on the parameters μ and p_θ. The addition of perturbations will cause p_θ to vary in time whilst μ remains, of course, fixed.

For a given physical system μ is a constant and p_θ is easily changed by providing different initial conditions. The qualitative structure of the phase portraits for the system (2.7a, b) depend on μ and p_θ. To determine these, the dependence of the equilibrium configurations of ϕ on μ and p_θ, and their stability, must be determined. From (2.7a) one immediately obtains the obvious condition that $\dot{\phi} = p_\phi = 0$ must hold for an equilibrium. The equilibrium condition from (2.7b) is satisfied by either

$$\sin\bar{\phi} = 0 \Rightarrow \bar{\phi} = 0, \pi \tag{2.8a}$$

or

$$1 - \cos\bar{\phi}\left(p_\theta/\left(\mu + \sin^2\bar{\phi}\right)\right)^2 = 0. \tag{2.8b}$$

Expression (2.8b) is equivalent to

$$1 - \dot{\theta}^2 \cos\bar{\phi} = 0 \tag{2.8c}$$

and is more easily solved in that form. Since $\phi = \bar{\phi} =$ constant at an equilibrium, eq. (2.7c), (2.8c), or physical insight, indicates that $\dot{\theta} = p_\theta/(\mu + \sin^2\bar{\phi}) = \bar{\dot{\theta}} =$ constant also must hold for an equilibrium. Hence one obtains

$$\bar{\phi} = \pm\cos^{-1}\left(1/\bar{\dot{\theta}}^2\right) \tag{2.9}$$

for the nontrivial equilibria of the system. For $\bar{\dot{\theta}} < 1$ these do not exist and it is easily shown that $\phi = 0$ is a stable center for $\bar{\dot{\theta}} < 1$. At $\bar{\dot{\theta}} = 1$ a pitchfork bifurcation [9] occurs and as $\bar{\dot{\theta}}$ is increased above 1 the two branches of (2.9) appear as symmetrically placed stable equilibria and $\phi = 0$ becomes a saddle point.

The dependence of $\bar{\phi}$ on p_θ is actually of more interest and is easily obtained by inverting (2.8b) to isolate p_θ as a function of $\bar{\phi}$. This indicates that $p_\theta = \mu$ is the critical condition for the appearance of nontrivial $\bar{\phi}$; this is equivalent to $\bar{\dot{\theta}} = 1$.

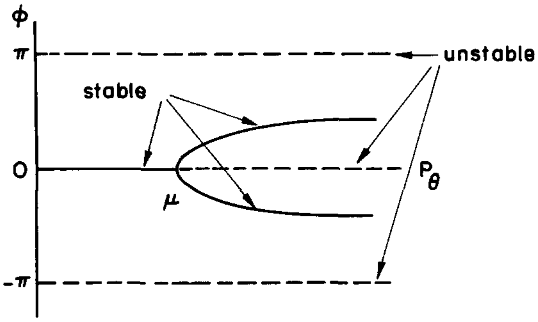

Fig. 2. Dynamic equilibria vs. p_θ.

A summary plot of the equilibria dependence on p_θ is given in fig. 2. Fig. 3 shows phase portraits, p_ϕ vs. ϕ, for various initial energy levels with p_θ held fixed. Fig. 3a is for the case $p_\theta < \mu$, the behavior is equivalent to that of the simple pendulum. Fig. 3b indicates the post-critical phase portrait, i.e., for $p_\theta > \mu$. Fig. 3c schematically shows how the family of phase portraits depends on p_θ, only the equilibria and some of the homoclinic motions are shown. This picture is a precursor for the three-dimensional Poincaré map [9] to be used when the perturbations are added and p_θ begins to undergo slow variations.

The homoclinic motions shown are of two types: (I) the usual "pendulum-type" part connecting $\phi = \pi$ to itself (one going each way, clockwise and counterclockwise) and, in addition, (II) for $p_\theta > \mu$ the pendulum motion which is forward and backward time-asymptotic to $\phi = 0$. These homoclinic motions have the potential for producing at least two distinct types of chaos.

For notational purposes the two families of saddle points given by $(\phi, p_\phi, p_\theta) = (\pi, 0, p_\theta)$ and $(\phi, p_\phi, p_\theta) = (0, 0, p_\theta > \mu)$ will be individually denoted by $\gamma_\pi(p_\theta)$ and $\gamma_0(p_\theta)$ respectively and collectively by $\gamma(p_\theta)$ in the following. Also, a homoclinic orbit associated with a particular $\gamma(p_\theta)$ will be written $q(t, p_\theta)$. Also, to distinguish the two types of unperturbed homoclinics the following labelling will be employed:

pendulum type homoclinics – Type I,
Duffing type homoclinics – Type II.
See fig. 3c.

The text by Nayfeh and Mook presents this unperturbed system as an exercise but overlooks the post-critical nontrivial equilibria by neglecting the inertia of the frame (exercises 2.9 and 2.10 in [10]).

2.2. *The perturbed system*

The perturbations to be considered here will be assumed small and include: (1) viscous damping in the bearings of the frame with associated damping constant c_θ, (2) viscous damping at the pendulum pivot with associated constant c_ϕ, (3) a constant torque T_0 applied to the frame about the vertical axis and (4) an oscillating torque $T_1 \sin(\omega t)$ applied to the frame, also about the vertical axis. These were chosen since they are typical of disturbances which might exist in an experimental set-up. Others can be chosen, of course, and the following analysis goes through directly as long as the perturbations do not depend on θ. If they are allowed to depend on θ in a periodic manner, but not on time, an equivalent formulation can be used [11] for predicting chaos, this is done in section 5.

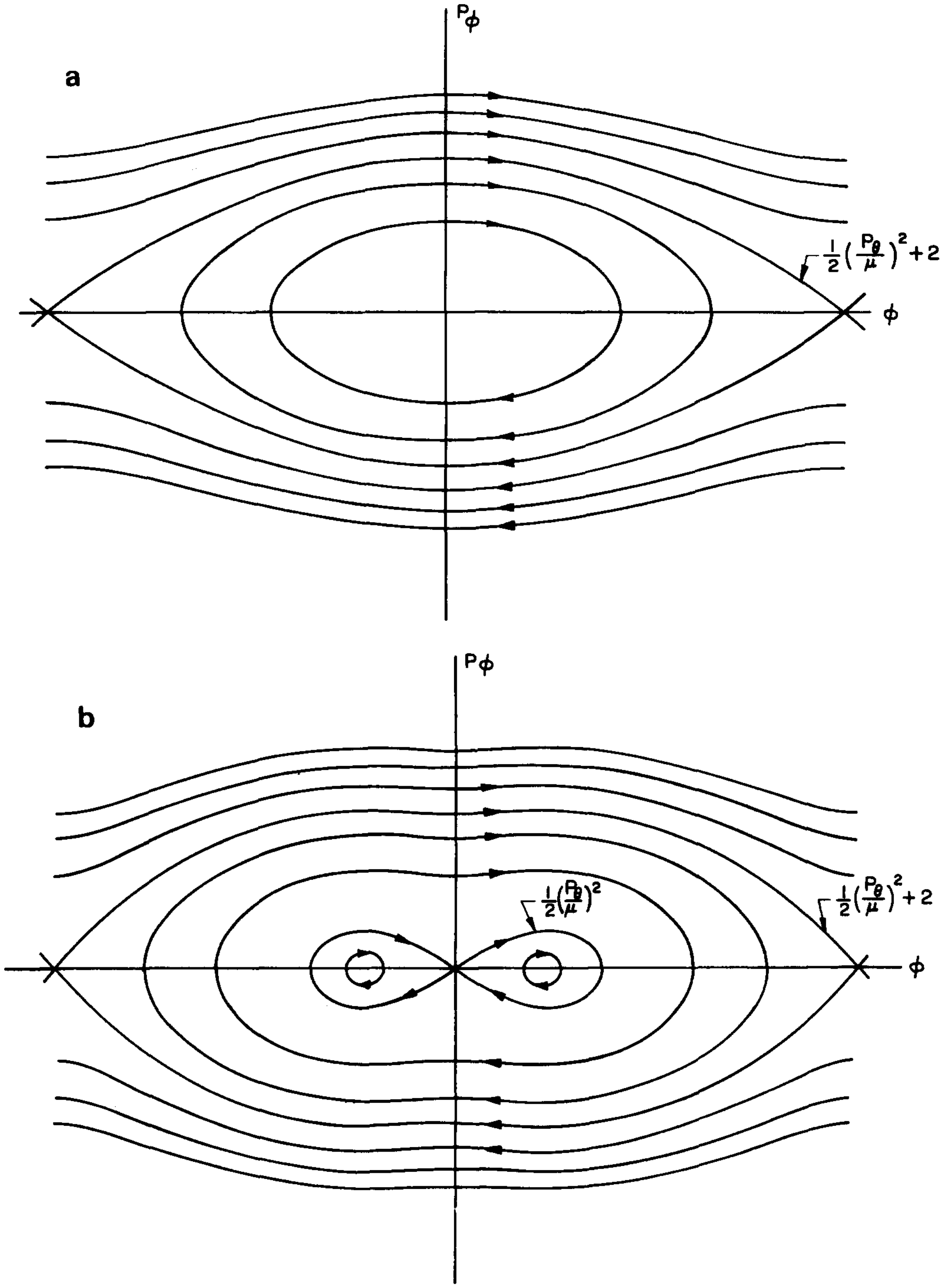

Fig. 3. Phase portraits, p_ϕ vs. ϕ. (a) $p_\theta < \mu$, (b) $p_\theta > \mu$, (c) stable and unstable manifolds of the saddle points vs. p_θ.

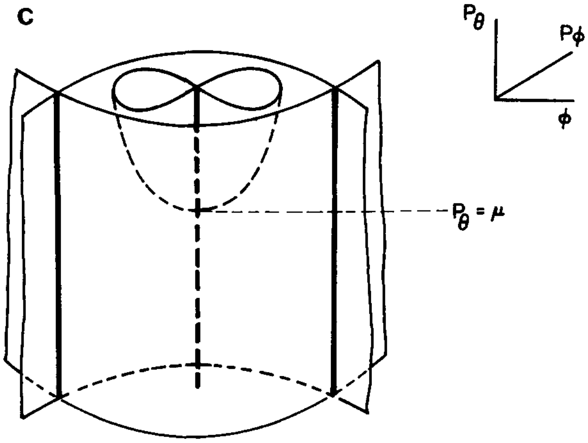

Fig. 3. Continued

Retaining their first order form, the perturbed equations of motion can be written as

$$\dot{\phi} = p_\phi, \tag{2.10a}$$

$$\dot{p}_\phi = \sin\phi\left[-1 + p_\theta^2 \cos\phi/\left(\mu + \sin^2\phi\right)^2\right] + \varepsilon Q_\phi(p_\phi), \tag{2.10b}$$

$$\dot{\theta} = p_\theta/\left(\mu + \sin^2\phi\right), \tag{2.10c}$$

$$\dot{p}_\theta = \varepsilon Q_\theta(\phi, p_\theta, t), \tag{2.10d}$$

where $Q_\phi = -c_\phi p_\phi$ and $Q_\theta = -c_\theta p_\theta/(\mu + \sin^2\phi) + T_0 + T_1 \sin(\omega t)$ represent the generalized forces not derivable from the potential $V(\phi)$ [12, 13].

The form of these equations is quite interesting, (2.10a, b) are of the form of a weakly damped oscillator with a particular form of parametric excitation. This small excitation is applied through the p_θ term in (2.10b) and is governed by its own differential equation, (2.10d). Hence (2.10a, b, d) form a slowly varying oscillator [1, 2].

For $\varepsilon = 0$, the physical system is represented by a one-parameter family of simple conservative oscillators. For $0 < \varepsilon \ll 1$ the structure of the phase space becomes more complicated in two significant ways. One change comes about due to the slow variation in p_θ, this necessitates extending the system to three time-dependent variables: (ϕ, p_ϕ, p_θ). Secondly, the fact that Q_θ depends explicitly on time means that the $\varepsilon \neq 0$ system dynamics are governed by a *third order nonautonomous* set of ordinary differential equations and hence a four-dimensional extended phase space is required. The fact that Q_θ is periodic in time is an important feature of these equations.

As is standard, the time $T = 2\pi/\omega$ Poincaré map is defined as follows [9]. Consider a point, the initial condition, given by $(\phi(t_0), p_\phi(t_0), p_\theta(t_0))$. Following its evolution in time, after one forcing period this point has evolved to $(\phi(t_0 + T), p_\phi(t_0 + T), p_\theta(t_0 + T))$. Without loss of generality t_0 can be taken to be zero and the Poincaré map is defined as

$$\boldsymbol{P}\colon \left(\phi(0), p_\phi(0), p_\theta(0)\right) \to \left(\phi(T), p_\phi(T), p_\theta(T)\right). \tag{2.11}$$

The dynamics are thus studied by considering iterates of this three-dimensional mapping.

Certain features of the unperturbed system are preserved for $0 < \varepsilon \ll 1$, details of the following observations can be found in [1, 2, 14, 15].

Firstly, hyperbolic equilibria become small amplitude periodic motions for $0 < \varepsilon \ll 1$, ε sufficiently small. However, in this system the equilibria, as considered in (ϕ, p_ϕ, p_θ) space, have a zero eigenvalue associated with the p_θ direction, making them nonhyperbolic. The perturbing forces combine in a manner such that only some of the equilibria are preserved. The conditions for these are determined by averaging the p_θ equation, (2.10d), along the unperturbed equilibria, over one period T and requiring the averaged system to have an equilibrium. Defining

$$\bar{Q}_\theta(\phi, p_\theta) = \frac{1}{T}\int_0^T Q_\theta(\phi, p_\theta, t)\,\mathrm{d}t = -c_\theta p_\theta/\mu + T_0, \tag{2.12}$$

where $\phi = \bar{\phi} = 0$ or π depending on which homoclinic is being considered. Setting $\bar{Q}_\theta = 0$ one obtains

$$T_0 = c_\theta p_\theta/\mu \quad \left(= c_\theta\dot{\theta} \quad \text{at } \phi = 0 \text{ or } \pi\right) \tag{2.13}$$

as the condition for a periodic motion to persist near $\bar{\phi} = 0$ or π for $0 < \varepsilon \ll 1$. Expression (2.13) simply states that the constant torque T_0 and the dissipative torque at the saddle point, $c_\theta\dot{\theta}$, must balance to first order. This agrees with intuitive expectations for a periodic motion; given values for T_0 and c_θ eq. (2.13) sets the nominal p_θ value at which periodic motions will exist. It should be noted that $\gamma(p_\theta)$, the curves of equilibria in (ϕ, p_ϕ, p_θ) space for $\varepsilon = 0$, perturb, for $0 < \varepsilon \ll 1$, into invariant, one-dimensional, time-periodic manifolds. To first order, the flow along these is governed by eqs. (2.10) evaluated on $\gamma(p_\theta)$. This flow is slow, in fact of $\mathcal{O}(\varepsilon)$, between the periodic motions which exist at the p_θ satisfying (2.13).

The periodic motions at $\bar{p}_\theta = \mu T_0/c_\theta$ are represented by fixed points for the map $\boldsymbol{P}$, these are denoted by $\tilde{\gamma}_\varepsilon(\bar{p}_\theta)$ or simply $\tilde{\gamma}_\varepsilon$. In the case when the original unperturbed equilibrium, $\gamma(\bar{p}_\theta)$, is of the saddle type in the (ϕ, p_ϕ) plane, the resulting periodic motion, $\gamma_\varepsilon(\bar{p}_\theta)$, is also of saddle type and is represented by a saddle type fixed point, $\tilde{\gamma}_\varepsilon(\bar{p}_\theta)$, for $\boldsymbol{P}$. This saddle point has a one-dimensional unstable manifold $W^{\mathrm{u}}(\tilde{\gamma}_\varepsilon(\bar{p}_\theta))$ and a two-dimensional stable manifold $W^{\mathrm{s}}(\tilde{\gamma}_\varepsilon(\bar{p}_\theta))$, see fig. 4. The stable manifold has one slowly contracting direction associated with the slow p_θ behavior. The p_θ behavior of the map near the fixed point is approximately governed by the averaged equation which is easily constructed from (2.12).

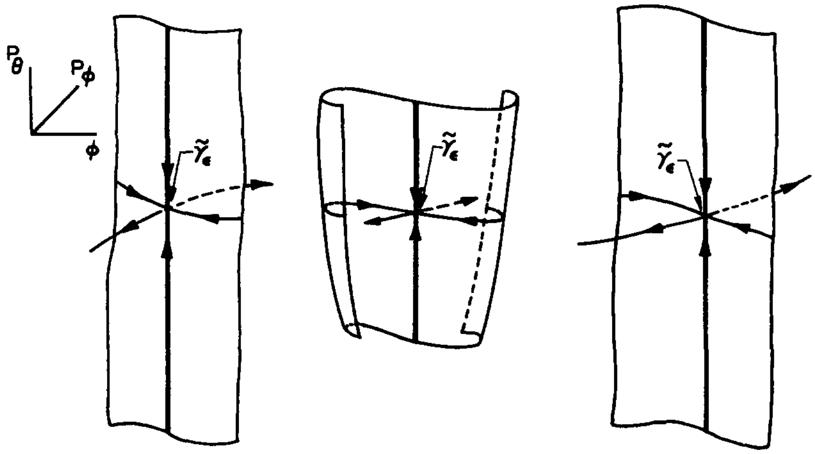

Fig. 4. The fixed points $\tilde{\gamma}_\varepsilon$ and their stable and unstable manifolds.

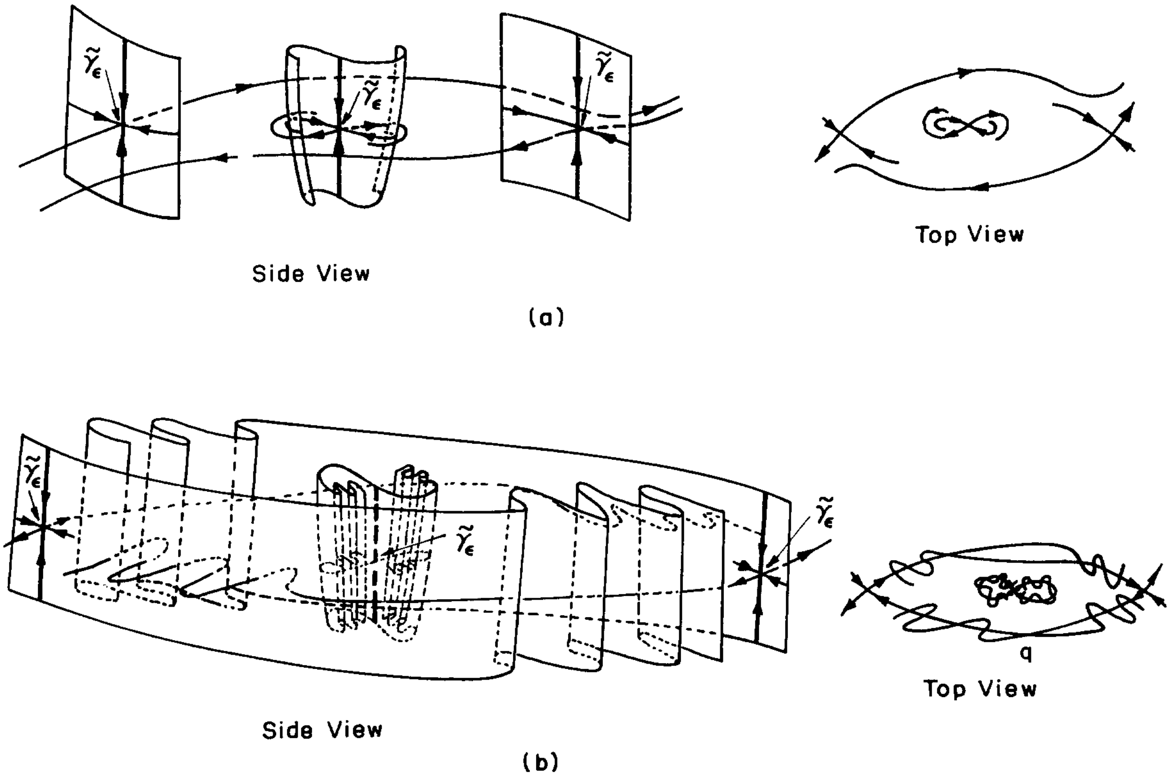

Fig. 5. (a) $W^u \cap W^s = \phi$. (b) $W^u \pitchfork W^s$.

These invariant manifolds for the map $\boldsymbol{P}$ are $\mathcal{O}(\varepsilon)$ close to their unperturbed counterparts for the original flow over semi-infinite time intervals, see fig. 5. The existence of chaotic motions for this system depends on the occurrence of transverse homoclinic points for the perturbed Poincaré map. The following section provides a method for detecting such intersections and describes some of the associated complicated dynamics.

3. Melnikov's method and the existence of chaotic motions

Both one-parameter families of saddle points in fig. 3, $\phi = \pi$ and $\phi = 0$ ($p_\theta > \mu$), have coincident stable and unstable manifolds which form two-dimensional surfaces (the two dimensions can be parameterized by time, along a particular orbit, and p_θ). The influence of the perturbations is to disturb this coincidence in one of two generic ways, depending on the parameter values. The manifolds may pass by each other as depicted in fig. 5a, or they may intersect transversally as indicated in fig. 5b. Fig. 5b shows the nature of the winding and accumulation for W^u that must occur in this case (W^s behaves similarly but is difficult to include in the diagram). The existence of a point like q, where W^s and W^u intersect in a nontangent manner, guarantees the existence of chaotic dynamics for the system via the Smale–Birkhoff homoclinic theorem [9]. Points such as q are termed *transverse homoclinic points* and are forward and backward asymptotic to the saddle point $\tilde{\gamma}_\varepsilon(\bar{p}_\theta)$ under iterates of $\boldsymbol{P}$. This follows directly from the invariance of $W^s(\tilde{\gamma}_\varepsilon(\bar{p}_\theta))$ and $W^u(\tilde{\gamma}_\varepsilon(\bar{p}_\theta))$.

In order to detect the existence of such transverse homoclinic orbits, a version of Melnikov's method is used. For more details on Melnikov's method as developed for slowly varying oscillators, see [1, 2]. The main idea is to follow $W^s(\tilde{\gamma}_\varepsilon(\bar{p}_\theta))$ and $W^u(\tilde{\gamma}_\varepsilon(\bar{p}_\theta))$ and measure, to first order in ε, the separation between them. This is done by using first order variational equations around the unperturbed homoclinic orbit, $q(t, \bar{p}_\theta)$, based at the saddle point $\gamma(\bar{p}_\theta)$ and by using these equations to formulate a distance function, $d(\alpha)$, which measures the separation. This distance function depends on a phase variable, α, that parameterizes the unperturbed homoclinic orbit, i.e., it is essentially a time variable. The distance function also provides information about the relative orientation of W^s and W^u. When $d(\alpha)$ is positive (negative) W^s is "inside" ("outside") of W^u, i.e., at time $t=\alpha$ W^s is closer to (further from) the unperturbed center around which $q(t, \bar{p}_\theta)$ passes. If there exists an α, say $\bar{\alpha}$, such that $d(\bar{\alpha})=0$ and $\partial d/\partial\alpha\,(\bar{\alpha}) \neq 0$, i.e., $d(\alpha)$ has a simple zero, then at $t=\bar{\alpha}$ W^s and W^u intersect transversally [1, 2, 9]. One such intersection implies, via the invariance of W^s and W^u, the following: (1) the existence of infinitely many such intersections and (2) the existence of three-dimensional horseshoes for the map $\boldsymbol{P}$, which in turn implies the existence of (a) infinitely many unstable periodic motions of arbitrarily long periods, and (b) infinitely many unstable nonperiodic, i.e., chaotic, motions.

The distance function $d(\alpha)$ can be formulated in such a manner that it is relatively easily computed. The calculation involves first order variations of the unperturbed stable and unstable manifolds due to the perturbations, see [1–3, 6, 9, 11, 13] for details and other examples. The Melnikov function, $M(\alpha)$, is related to $d(\alpha)$ as follows:

$$d(\alpha)=\frac{\varepsilon M(\alpha)}{\left|\left(\frac{\partial H}{\partial p_\phi}(q(-\alpha,\bar{p}_\theta))\right)^2+\left(\frac{\partial H}{\partial \phi}(q(-\alpha,\bar{p}_\theta))\right)^2\right|^{1/2}}+\mathcal{O}(\varepsilon^2), \tag{3.1}$$

and is, for our example, given by

$$M(\alpha)=\int_{-\infty}^{\infty}\left[\frac{\partial H}{\partial p_\phi}Q_\phi+\frac{\partial H}{\partial p_\theta}Q_\theta\right]\{q(t,\bar{p}_\theta),t+\alpha\}\,\mathrm{d}t-\frac{\partial H}{\partial p_\theta}(\gamma(\bar{p}_\theta))\int_{-\infty}^{\infty}Q_\theta(q(t,\bar{p}_\theta),t+\alpha)\,\mathrm{d}t. \tag{3.2}$$

The { } bracketed term indicates that the functions in the integrals are to be evaluated along the unperturbed homoclinic orbit at $p_\theta=\bar{p}_\theta$, $q(t,\bar{p}_\theta)$, and that the explicitly time-dependent terms are to be evaluated at time $t+\alpha$. This formulation is not the most general for slowly varying oscillators, the reader should see refs. [1, 2] for a general and thorough treatment. For the following results $\bar{p}_\theta>\mu$ must hold.

From eq. (3.1) it is seen that for ε sufficiently small, the nature of $M(\alpha)$ captures that of the distance function, $d(\alpha)$. Specifically, if $M(\alpha)$ has simple zeros, $d(\alpha)$ will also (for small ε). In addition, the transitions from no zeros, to tangent zeros, to simple zeros of $d(\alpha)$ is mimicked by $M(\alpha)$, i.e., global bifurcations involving homoclinic tangencies can be captured by $M(\alpha)$ [9].

The form of $M(\alpha)$ given in (3.2) is rather unenlightening, a more understandable presentation is found by substituting in for the Q's and the $\partial H/\partial p$ terms:

$$\begin{aligned}M(\alpha)=&\int_{-\infty}^{\infty}\left[-c_\phi\dot{\phi}^2+\dot{\theta}\left(-c_\theta\dot{\theta}+T_0+T_1\sin(\omega(t+\alpha))\right)\right]\{q(t,\bar{p}_\theta),t+\alpha\}\,\mathrm{d}t\\&-\frac{T_0}{c_\theta}\int_{-\infty}^{\infty}\left(-c_\theta\dot{\theta}+T_0+T_1\sin(\omega(t+\alpha))\right)]\left(q(t,\bar{p}_\theta),t+\alpha\right)\mathrm{d}t,\end{aligned} \tag{3.3}$$

where $\dot{\phi}$ and $\dot{\theta}$ should, at least formally, be replaced by p_ϕ and $p_\theta/(\mu + \sin^2\phi)$ respectively. However from a theoretical viewpoint it is easier to treat $M(\alpha)$ in the above form.

It is convenient to rewrite $M(\alpha)$ as follows:

$$\begin{aligned} M(\alpha) &= -c_\phi I_1 - c_\theta I_2 + T_1 I_3(\omega, \alpha), \\ I_1 &= \int_{-\infty}^{\infty} [\dot{\phi}^2](q(t, \bar{p}_\theta))\,\mathrm{d}t, \\ I_2 &= \int_{-\infty}^{\infty} \left[\dot{\theta} - T_0/c_\theta\right]^2 (q(t, \bar{p}_\theta))\,\mathrm{d}t, \\ I_3(\omega, \alpha) &= \int_{-\infty}^{\infty} \left[-T_0/c_\theta + \dot{\theta}\right] \sin(\omega(t+\alpha))(q(t, \bar{p}_\theta), t+\alpha)\,\mathrm{d}t. \end{aligned} \tag{3.4}$$

The integral I_1 is well behaved since $\dot{\phi}$ approaches zero exponentially fast at both ends ($t \to \pm\infty$) of the unperturbed homoclinic motion $q(t, \bar{p}_\theta)$. Integral I_2 has potential convergence problems since $\dot{\theta} \to$ constant as $t \to \pm\infty$ along $q(t, \bar{p}_\theta)$ but is rescued by employing the condition $\bar{p}_\theta = \mu T_0/c_\theta$ which implies that $\dot{\theta}$ approaches T_0/c_θ as $t \to \pm\infty$ along $q(t, \bar{p}_\theta)$. The integral $I_3(\omega, \alpha)$ can be further simplified in two steps. The following analysis holds for both types of homoclinic motions. First we deal with the $-T_0/c_\theta$ term in the integral. Expanding $\sin(\omega(t+\alpha))$ and evaluating the improper integral as a limit of a sequence of proper integrals gives

$$\begin{aligned} &\int_{-\infty}^{\infty} \frac{T_0}{c_\theta} \sin(\omega(t+\alpha))\,\mathrm{d}t \\ &\quad = \lim_{i\to\infty} \left[\frac{T_0}{c_\theta} \cos\omega\alpha \int_{-2\pi i/\omega}^{2\pi i/\omega} \sin\omega t\,\mathrm{d}t + \frac{T_0}{c_\theta} \sin\omega\alpha \int_{-2\pi i/\omega}^{2\pi i/\omega} \cos\omega t\,\mathrm{d}t\right] = 0. \end{aligned} \tag{3.5}$$

Next we deal with the $\dot{\theta}\sin\omega(t+\alpha)$ term in the integral. First, one notes that $\dot{\theta}$ is an even function of t on $q(t, p_\theta)$ if $t = 0$ is taken to be at the "midpoint" of $q(t, p_\theta)$. Then by expanding $\sin(\omega(t+\alpha)) = \sin(\omega t)\cos(\omega\alpha) + \cos(\omega t)\sin(\omega\alpha)$, the odd part of the integrand, $\dot{\theta}\sin(\omega t)\cos(\omega\alpha)$, can be eliminated since it integrates to zero. The remaining term, $\dot{\theta}\cos(\omega t)\sin(\omega\alpha)$, is still only conditionally convergent in the integral. It is computed by considering the integral as a limit and integrating once by parts as follows:

$$I_3(\omega, \alpha) = \sin(\omega\alpha) \lim_{\tau_i\to\infty} \left[\left.\frac{\dot{\theta}\sin(\omega t)}{\omega}\right|_{-\tau_i}^{\tau_i} - \frac{1}{\omega}\int_{-\tau_i}^{\tau_i} [\ddot{\theta}\sin(\omega t)]\{q(t, \bar{p}_\theta)\}\,\mathrm{d}t\right]. \tag{3.6a}$$

By choosing the sequence of times $\tau_i = 2\pi i/\omega$, letting $i(=1,2,3,\ldots) \to \infty$, and using (3.5) one finally obtains

$$\begin{aligned} I_3(\omega, \alpha) &= \sin(\omega\alpha)\bar{I}_3(\omega), \\ \bar{I}_3(\omega) &= \frac{-1}{\omega}\int_{-\infty}^{\infty} [\ddot{\theta}\sin(\omega t)](q(t, \bar{p}_\theta))\,\mathrm{d}t. \end{aligned} \tag{3.6b}$$

$\bar{I}_3(\omega)$ is well behaved; the acceleration of the frame, $\ddot{\theta}$, is an odd function of time and approaches zero exponentially as $t \to \pm\infty$ on $q(t, \bar{p}_\theta)$. Thus the desired form of $M(\alpha)$ is given by

$$M(\alpha) = -c_\phi I_1 - c_\theta I_2 + T_1 \bar{I}_3(\omega)\sin(\omega\alpha). \tag{3.7}$$

The general behavior of $M(\alpha)$ is now apparent. For fixed parameter values $(\mu, c_\phi, c_\theta, T_0, T_1, \omega)$ the terms $-(c_\phi I_1 + c_\theta I_2)$ and $T_1 \bar{I}_3(\omega)$ are constant. Hence, as α is varied $M(\alpha)$ oscillates about a mean value of $-(c_\phi I_1 + c_\theta I_2)$ in a harmonic manner with an amplitude of $T_1 \bar{I}_3(\omega)$. It is quite simple to then determine the general relative behavior of $W^s(\tilde{\gamma}_\varepsilon(\bar{p}_\theta))$ and $W^u(\tilde{\gamma}_\varepsilon(\bar{p}_\theta))$.

It is obvious that $I_1 > 0$ since $\dot{\phi}$ is not everywhere zero along a homoclinic motion. Similarly, we have $I_2 > 0$. (The sign of $\bar{I}_3(\omega)$ is of no consequence since it is simply a term in the amplitude of an oscillating function.)

Now for $T_1 = 0$ (no oscillatory input) $M(\alpha)$ is identically zero if

$$\left(\frac{c_\phi}{c_\theta}\right) = -\left(\frac{I_2}{I_1}\right) \ (>0).$$

Thus for c_ϕ and c_θ of opposite sign, the system possesses a homoclinic motion. The situation, for $T_1 = 0$, is as follows:

$$\left(\frac{c_\phi}{c_\theta}\right) < -\left(\frac{I_2}{I_1}\right) \to M(\alpha) > 0, \qquad W^u\text{“outside” } W^s; \tag{3.8a}$$

$$\left(\frac{c_\phi}{c_\theta}\right) = -\left(\frac{I_2}{I_1}\right) \to M(\alpha) = 0, \qquad W^u \text{ and } W^s \text{ coincident}; \tag{3.8b}$$

$$\left(\frac{c_\phi}{c_\theta}\right) > -\left(\frac{I_2}{I_1}\right) \to M(\alpha) < 0, \qquad W^u\text{“inside” } W^s. \tag{3.8c}$$

(The condition (3.8b) is valid to order ε.) Case (3.8a) indicates that if c_ϕ/c_θ is sufficiently small, the pendulum motion will escape beyond $q(t, \bar{p}_\theta)$ for initial conditions near the saddle point $\bar{\phi}$. For the $\bar{\phi} = \pi$ homoclinic (Type I) this implies that sustained motions involving the pendulum swinging over the top can occur. For the $\bar{\phi} = 0$ homoclinic (Type II) it implies that motions can achieve steady-state amplitudes above the maximum displacement on the associated $q(t, \bar{p}_\theta)$, these may also potentially end up as sustained rotational motions. If condition (3.8c) holds the motions are “swept inside” of $q(t, \bar{p}_\theta)$ and typically end up at lower amplitudes. For the $\bar{\phi} = \pi$ homoclinics (I) this implies that the system will settle down to either a periodic or steady nonrotational motion and for the $\bar{\phi} = 0$ homoclinics (II) it means that the motion will settle down to some type of an oscillatory or, more likely, a steady motion near $\phi = \bar{\phi}$ given by eq. (2.9).

The above general discussion is summarized in fig. 6. In the figure it has been assumed that $(-I_2/I_1)_{\mathrm{I}} > (-I_2/I_1)_{\mathrm{II}}$, the other case is similar and is easily worked out. Also, in this case $(T_1 = 0)$ the system is autonomous and thus the invariant manifolds shown are for the differential equation, *not* for the map $\boldsymbol{P}$. Similarly the points $\bar{\phi} = 0$, π, $\cos^{-1}(1/\bar{\dot{\theta}})$ are equilibria, not periodic motions; this is so since there is no periodic input.

For $T_1 \neq 0$ the sequence of diagrams in fig. 6 is complicated by several things. Firstly, the system becomes nonautonomous and thus all figures must be interpreted in terms of the discrete time map $\boldsymbol{P}$. Also, the homoclinic bifurcations depicted in figs. 6b, d each split into a *pair* of homoclinic tangencies, i.e., two global bifurcations must occur to go from fig. 6a to 6c and two more must occur for the 6c to 6e transition. (In reality infinitely many bifurcations occur as one passes through a homoclinic tangency, here only the primary global bifurcations are considered [4, 9].)

The homoclinic tangencies occur near $(\mathcal{O}(\varepsilon))$ the points where $M(\alpha)$ has tangent zeros. These occur when the magnitudes of the mean value of $M(\alpha)$, $|c_\phi I_1 + c_\theta I_2|$, and the oscillatory amplitude, $|T_1 \bar{I}_3(\omega)|$,

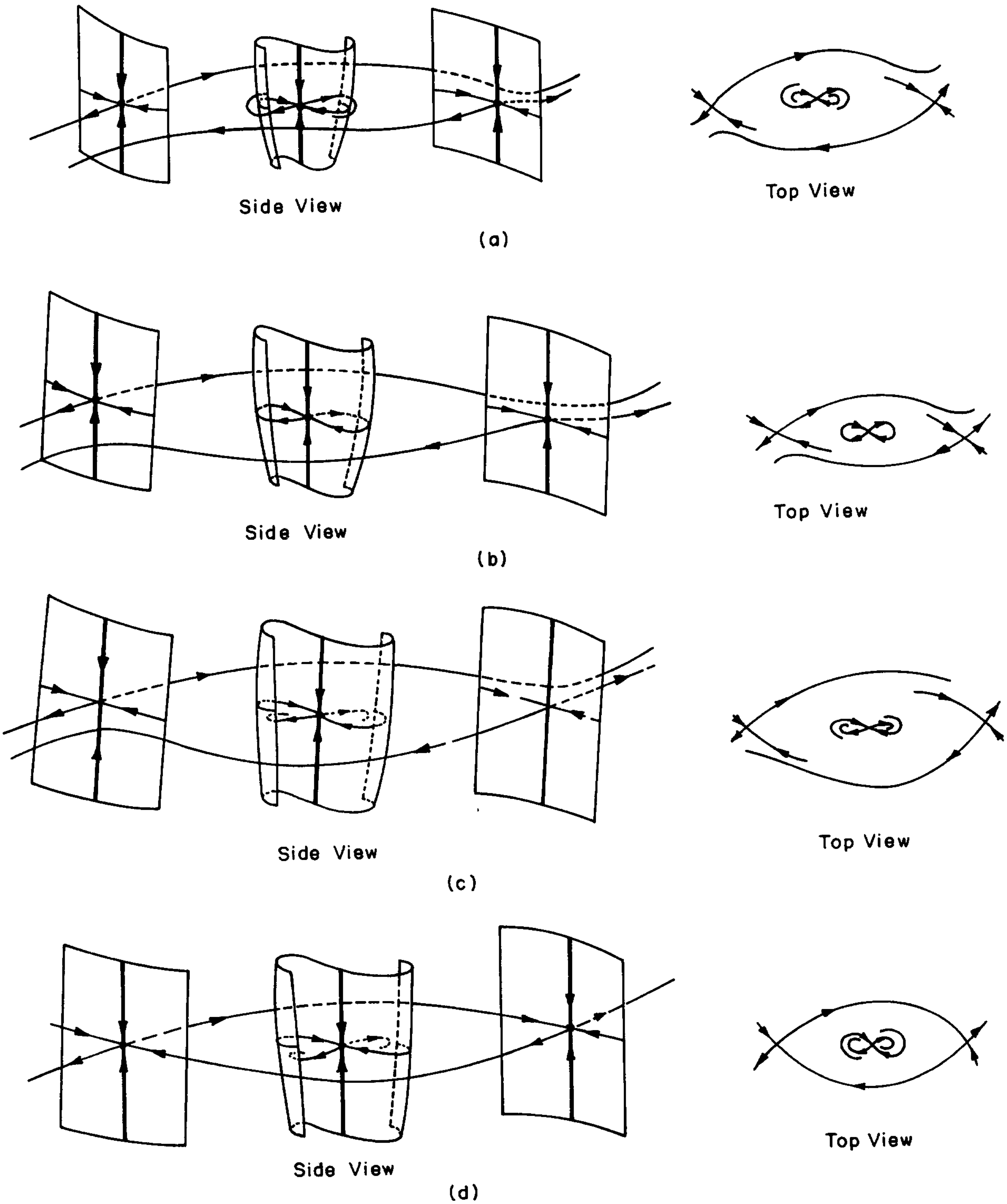

Fig. 6a–e. The autonomous case, $T_1 = 0$. (See fig. 7 also.) (a) Case (3.8a) for I and II. (b) Case (3.8a) for I, (3.8b) for II. (c) Case (3.8a) for I, (3.8c) for II. (d) Case (3.8b) for I, (3.8c) for II. (e) Case (3.8c) for I and II.

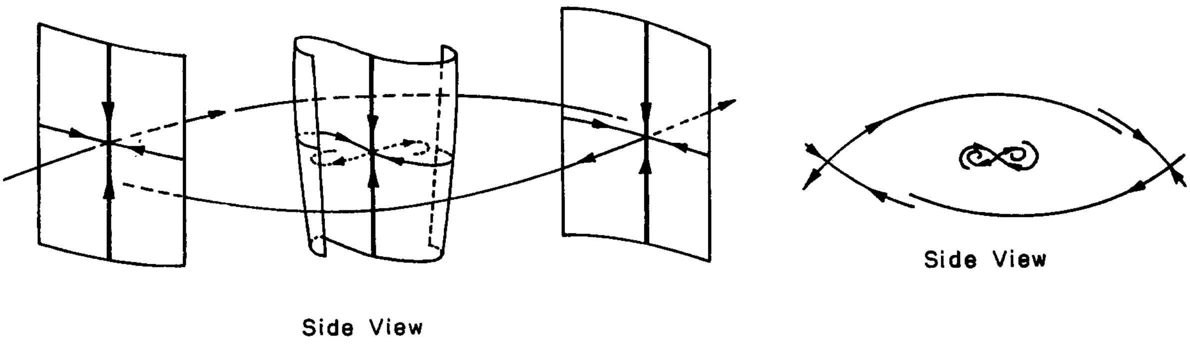

(e)

Fig. 6. Continued

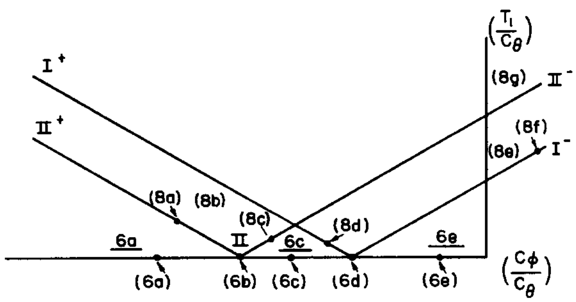

Fig. 7. Bifurcation diagram for $T_1 \neq 0$, the nonautonomous case.

are equal: i.e., at a driving amplitude of

$$T_1^* = \left| \frac{c_\phi I_1 + c_\theta I_2}{\bar{I}_3(\omega)} \right|. \tag{3.9}$$

Fig. 7 shows the homoclinic bufurcation diagram assuming $(-I_2/I_1)_{\mathrm{I}} > (-I_2/I_2)_{\mathrm{II}}$. Bifurcation "wedges" emerge from the autonomous homoclinic points and chaotic dynamics are possible at parameter values interior to these wedges. For $T_1 \neq 0$ the behavior at parameter values exterior to the wedges is very similar to the corresponding $T_1 = 0$ behavior; however, the system is nonautonomous and thus fixed points represent periodic motions, etc. In fig. 7 for $T_1 \neq 0$ the portions of fig. 6 previously referred to are now underlined to remind the reader that the diagrams must be properly interpreted in terms of $\boldsymbol{P}$. Fig. 8 depicts the remaining, and more interesting cases from fig. 7.

Several interesting dynamic behaviors are possible. For instance, inside the wedge II, chaotic motions are possible in which the pendulum erratically swings back and forth past $\phi = 0$, but not over the top; this is very much like the chaos observed in Duffing's equation [3, 4, 7]. Inside the wedge I chaotic motions exist in which the pendulum undergoes arbitrary sequences of clockwise and counterclockwise rotations about $\phi = \pi$ [5, 6, 13, 16]. This example provides two distinct types of chaotic motions commonly studied. In fact, in the region where the interiors of both wedges intersect, both types of chaos are simultaneously possible. The dynamics in that region have the potential for the system "hopping" from one type of chaos

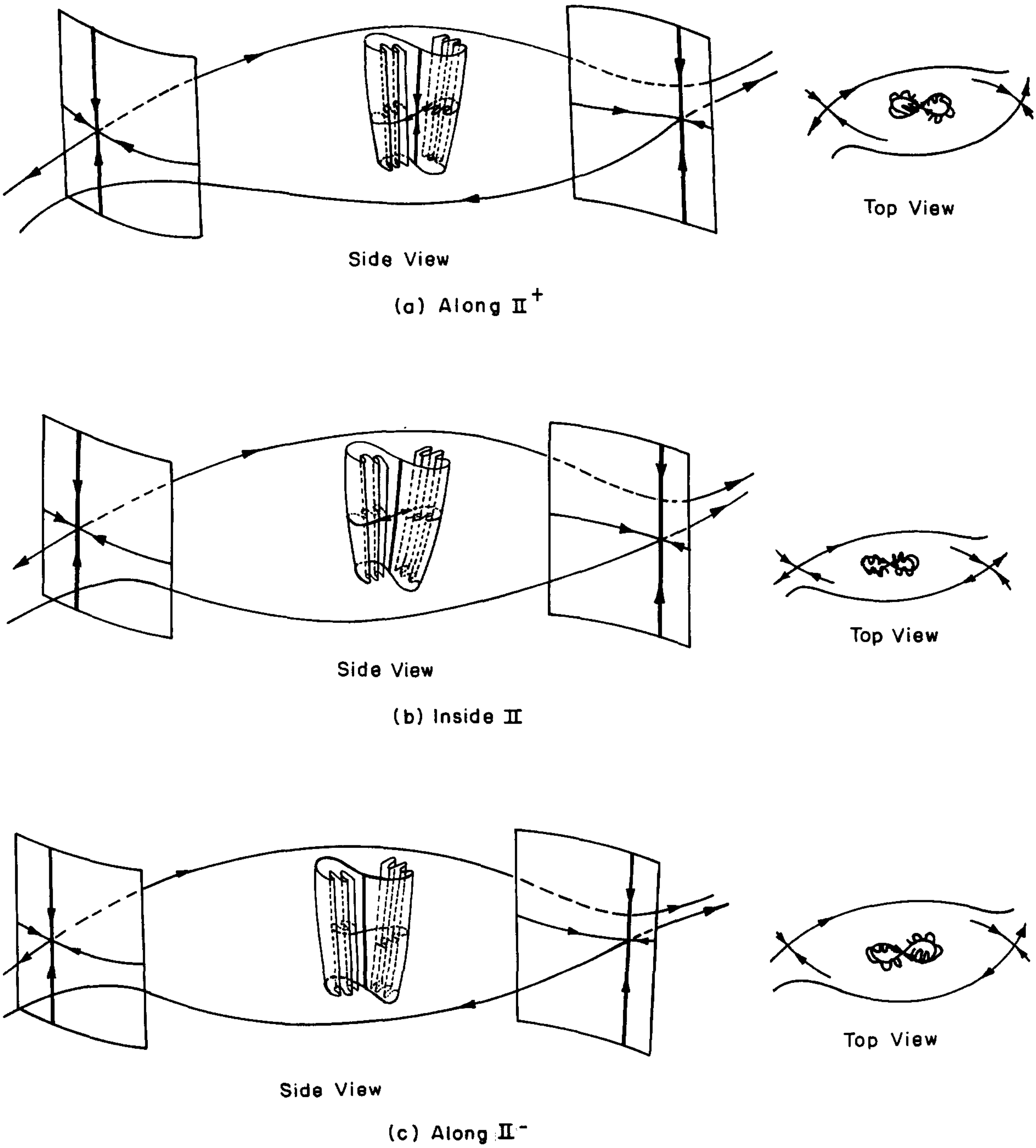

Fig. 8a–g. Structures of the invariant manifolds (refer to fig. 7).

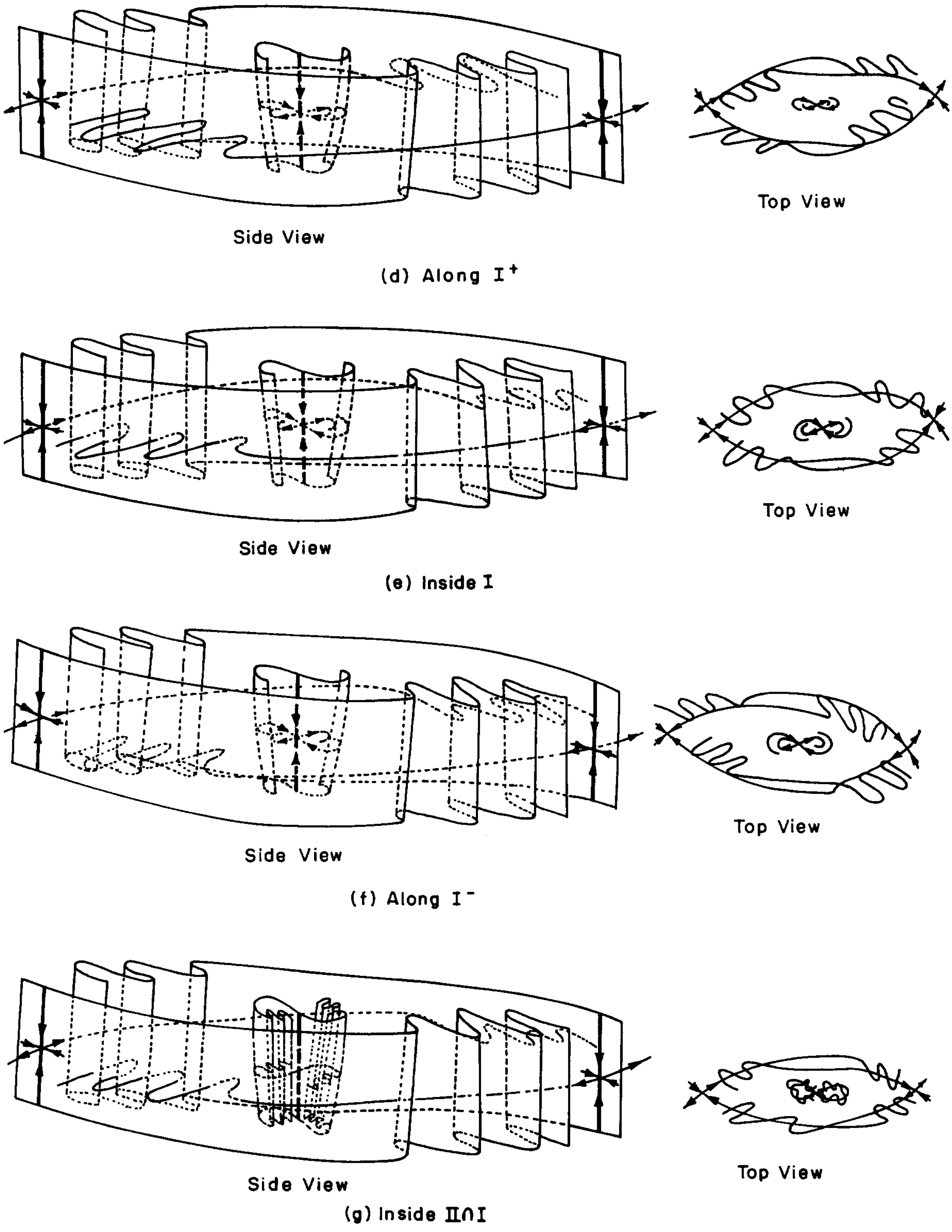

Fig. 8. Continued

to another; this cannot be proved using the present methods since the invariant manifolds for the two types of chaos remain bounded away from one another. However, for $\bar{p}_\theta = \mathcal{O}(1/\varepsilon^2)$ it may be possible to predict, using methods similar to the present ones, when these manifolds mingle thus proving the existence of such "hopping."

The types of chaos which exist here involve arbitrary sequences of physically different events. For the pendulum type of chaos (I) there exist motions in which the pendulum swings through approximately full 2π revolutions in arbitrary clockwise and counterclockwise sequences. For the Duffing type of chaos (II) there exist motions which swing back and forth through $\phi = 0$ towards $\phi > 0$ and $\phi < 0$ in arbitrary orders. The proofs of these statements involve the use of symbol sequences and symbolic dynamics applied to the *hyperbolic Smale horseshoes* which exist when W^s and W^u intersect transversally. See [2, 9, 13] for details.

The diagram of fig. 7 contains qualitative information about motions other than chaos. Similar reasoning as was used in the $T_1 = 0$ case indicates that, for example, sustained rotational motions are possible for parameter values to the left of wedge II. Other similar observations can be made as well.

It must be pointed out that a different bifurcation diagram must be considered if $(-I_2/I_1)_{\mathrm{II}} > (-I_2/I_1)_{\mathrm{I}}$. Essentially, the order of wedges I and II is switched and the sequences of bifurcations are changed. The details of that case can easily be worked out in the manner presented above.

4. A limiting case

Considered in this section is the case when the rotating frame is assumed to be massive in comparison with the pendulum: i.e., μ is large. In this case it is desired that $\dot{\theta}$ be a specified function of time, as compared with the torque which was specified in the above. This can be accomplished by allowing μ, T_0, c_θ, T_1 and p_θ to be large enough such that $\dot{\theta}$ is specified and the pendulum dynamics have an insignificant effect on the motion of the frame. In this case the applied torques will specify $\dot{\theta}$.

Eqs. (2.10) become a set of singularly perturbed equations of motion in this case, here only first order effects are considered. With μ, T_0, c_θ, T_1 and p_θ large, (2.10d) simplifies to (ε is, of course, removed)

$$\dot{p}_\theta \cong -c_\theta p_\theta/\mu + T_0 + T_1 \sin \omega t, \tag{4.1}$$

which has a steady state solution given by

$$p_\theta = \frac{\mu T_0}{c_\theta} + \frac{\mu^2 T_1}{\omega^2\mu^2 + c_\theta^2} \sin(\omega t + \Psi), \tag{4.2}$$

where Ψ is an inconsequential phase angle. In this case, $\mu \gg 1$ which implies $p_\theta \simeq \mu\dot{\theta}$ (from 2.4) and hence that $\dot{\theta}$ will follow p_θ according to

$$\dot{\theta} \cong \frac{p_\theta}{\mu} = \frac{T_0}{c_\theta} + \frac{\mu T_1}{\omega^2\mu^2 + c_\theta^2} \sin(\omega t + \Psi). \tag{4.3}$$

Now, $\dot{\theta} \cong p_\theta/\mu$ is the parametric excitation term in (2.10b) and is now a known time-dependent function. Here it is assumed that $\dot{\theta}$ can then be expressed as

$$\dot{\theta} = \Omega + \varepsilon\beta \sin(\omega t), \tag{4.4}$$

where $\Omega = T_0/c_\theta$, $\varepsilon\beta = \mu T_1/(\omega^2\mu^2 + c_\theta^2)$ and the phase angle Ψ is dropped without loss of generality. The system is now a single degree of freedom oscillator with weak parametric excitation and damping, the equations of motion are obtained by substituting (4.4) into (2.10a, b)

$$\dot{\phi} = p_\phi, \tag{4.5a}$$

$$\dot{p}_\phi = \sin\phi\left[-1 + \Omega^2\cos\phi\right] + \varepsilon\tilde{Q}_\phi + \mathcal{O}(\varepsilon^2), \tag{4.5b}$$

$$\tilde{Q}_\phi = -c_\phi p_\phi + 2\Omega\beta\sin\phi\cos\phi\sin(\omega t).$$

Here there is no advantage to using the p (momentum) variables; the second order form of the oscillator equation is (neglecting $\mathcal{O}(\varepsilon^2)$ terms)

$$\ddot{\phi} + (1 - \Omega^2\cos\phi)\sin\phi = \varepsilon\left[-c_\phi\dot{\phi} + 2\Omega\beta\sin\phi\cos\phi\sin(\omega t)\right]. \tag{4.6}$$

The unperturbed system ($\varepsilon = 0$) has Hamiltonian

$$\tilde{H}(\phi, p_\phi) = \frac{p_\phi^2}{2} + \frac{\Omega^2}{2}\sin^2\phi - \cos\phi \tag{4.7}$$

and unperturbed phase portraits equivalent to those in figs. 3a and 3b for $\Omega < 1$ and $\Omega > 1$ respectively. (Recall that $p_\phi = \dot{\phi}$.)

The usual planar Melnikov analysis [9] is applicable and gives a Melnikov function of

$$\tilde{M}(\alpha) = \int_{-\infty}^{\infty}\left[\frac{\partial\tilde{H}}{\partial p_\phi}\tilde{Q}_\phi\right]\{\tilde{q}(t), t+\alpha\}\,\mathrm{d}t \tag{4.8a}$$

$$= \int_{-\infty}^{\infty}\left[-c_\phi\dot{\phi}^2 + 2\Omega\beta\sin\phi\cos\phi\dot{\phi}\sin(\omega(t+\alpha))\right]\{\tilde{q}(t), t+\alpha\}\,\mathrm{d}t \tag{4.8b}$$

$$= -c_\phi\tilde{I}_1 + 2\Omega\beta\tilde{I}_2(\omega,\alpha), \tag{4.8c}$$

$$\tilde{I}_1 = \int_{-\infty}^{\infty}[\dot{\phi}^2]\{\tilde{q}(t)\}\,\mathrm{d}t,$$

$$\tilde{I}_2(\omega,\alpha) = \int_{-\infty}^{\infty}\left[\sin\phi\cos\phi\dot{\phi}\sin(\omega(t+\alpha))\right]\{\tilde{q}(t), t+\alpha\}\,\mathrm{d}t,$$

where $\tilde{q}(t)$ represents a homoclinic motion for the $\varepsilon = 0$ version of (4.5). $\tilde{I}_2(\omega,\alpha)$ can be simplified as was done in section 3, here it has a different form for each of the two sets of homoclinics. There are no convergence problems whatsoever since both $\sin\phi$ and p_ϕ approach zero exponentially fast as $t \to \pm\infty$ along any of the $\tilde{q}(t)$.

The global bifurcation result, where $\tilde{M}(\alpha)$ has tangent zeros, can be expressed as

$$\beta^* = \left|\frac{c_\phi\tilde{I}_1}{2\Omega\beta\bar{I}_2(\omega)}\right|. \tag{4.9}$$

$$\bar{I}_2(\omega) = \int_{-\infty}^{\infty}\left[p_\phi\sin\phi\cos\phi\sin(\omega t)\right]\{\tilde{q}(t)\}\,\mathrm{d}t.$$

The integral $\bar{\bar{I}}(\omega)$ is the nonvanishing amplitude of the $\tilde{I}_2(\omega,\alpha)$ term; it can be shown that $\tilde{I}_2(\omega,\alpha)=\bar{I}(\omega)\cos(\omega\alpha)$.

Here the possible dynamics are much less complicated. For positive c_ϕ, $\tilde{M}(\alpha)$ maintains a negative mean value and has no zeros, tangent zeros or simple zeros for $\beta<\beta^*$, $\beta=\beta^*$ (to $\mathcal{O}(\varepsilon)$) and $\beta>\beta^*$ respectively. The damped, unforced system has no homoclinic motions.

The qualitative features of the bifurcation diagram for this case are easily obtained from fig. 7. Letting c_θ, T_0, T_1, μ and p_θ become large, it is seen that T_1/c_θ remains finite and generally nonzero while (c_ϕ/c_θ) approaches zero. Thus the two wedges in fig. 7 are pushed together at the origin while their slopes remain finite and, in general, different. The diagrams referred to from figs. 6 and 8 again must be correlated to the present situation: a two-dimensional Poincaré map with saddle points having stable and unstable manifolds which are one-dimensional.

The discussion of this limiting case is closed here, there exist several examples of chaotic motions in forced, damped oscillators such as this one, the reader is referred to [3–7] and the references contained therein.

5. The case of spatially-periodic disturbances

In certain circumstances there may exist external disturbances which depend on the θ orientation of the pendulum; these are necessarily 2π periodic in θ. Examples of these include magnetic fields or aerodynamic loads from nonrotating components.

If the disturbances are not time-dependent, a formulation can be given in which the system recovers the form of a slowly varying oscillator. In general the equations can be written as

$$\dot{\phi}=p_\phi, \tag{5.1a}$$

$$\dot{p}_\phi=-\frac{\partial H}{\partial\phi}+\varepsilon\hat{Q}_\phi(\phi,p_\phi,\theta,p_\theta), \tag{5.1b}$$

$$\dot{\theta}=p_\theta/(\mu+\sin^2\phi)=\frac{\partial H}{\partial p_\theta}, \tag{5.1c}$$

$$\dot{p}_\theta=\varepsilon\hat{Q}_\theta(\phi,p_\phi,\theta,p_\theta), \tag{5.1d}$$

where $\hat{Q}_\phi$ and $\hat{Q}_\theta$ are 2π-periodic in θ and ϕ. It is now assumed that the system's θ-rotational direction does not reverse, i.e., that $\dot{\theta}$ is strictly positive (or strictly negative, it does not matter). A change of variables is then implemented, this transformation suppresses the time dependence of the dynamic variables and renders θ as the independent variable. Denoting $\mathrm{d}/\mathrm{d}\theta$ as $(\ )'$ eqs. (5.1) can be written with θ as the independent variable:

$$\phi'=p_\phi\Big/\left[\frac{\partial H}{\partial p_\theta}\right], \tag{5.2a}$$

$$p_\phi'=\left[-\frac{\partial H}{\partial\phi}+\varepsilon\hat{Q}_\phi\right]\Big/\left[\frac{\partial H}{\partial p_\theta}\right], \tag{5.2b}$$

$$\theta'=1, \tag{5.2c}$$

$$p_\theta'=\varepsilon\hat{Q}_\theta\Big/\left[\frac{\partial H}{\partial p_\theta}\right]. \tag{5.2d}$$

Here (5.2a, b, d) constitute a slowly varying oscillator, and (5.2c) is analogous to the equation $\dot{t} = 1$ for the case of time-dependent disturbances.

In this case Melnikov's method goes through exactly as before with eqs. (5.2) replacing (2.10) and θ replacing time. Hence, the Poincaré map is defined as follows:

$$\boldsymbol{P}_\theta: \left(\phi(0), p_\phi(0), p_\theta(0)\right) \to \left(\phi(2\pi), p_\phi(2\pi), p_\theta(2\pi)\right) \tag{5.3}$$

where the explicit argument of ϕ, p_ϕ and p_θ is θ. The unperturbed ($\varepsilon = 0$) phase space is, of course, topologically equivalent to that for the previous case; they will not be identical, however, due to the fact that the equations are divided by $\partial H/\partial p_\theta = p_\theta/(\mu + \sin^2\phi)$ and the level curves of H at each value of p_θ are now parametrized by θ instead of time. When the perturbation is "switched on" this structure breaks up in the same qualitative manner as in the time-dependent case.

The condition for an equilibrium to continue as a fixed point of $\boldsymbol{P}_\theta$ under the addition of perturbations is that the following θ-averaged system have an equilibrium:

$$\begin{aligned} p_\theta' &= \bar{\hat{Q}}_\theta(\phi, p_\phi, p_\theta), \\ \bar{\hat{Q}}_\theta &= \frac{1}{2\pi}\int_0^{2\pi} \hat{Q}_\theta(\phi, p_\phi, \theta, p_\theta)\, \mathrm{d}\theta. \end{aligned} \tag{5.4}$$

This again will lead to a condition which balances the external energy sources with dissipation to first order. The fixed points are again denoted by $\tilde{\gamma}_\varepsilon$ and the p_θ values at these are given by $\bar{p}_\theta$. The Melnikov integral for this case is then given by

$$\begin{aligned} M_\theta(\alpha) = &\int_{-\infty}^{\infty} \left[\frac{\partial H}{\partial p_\phi}\hat{Q}_\theta \Big/ \left(\frac{\partial H}{\partial p_\theta}\right) + \hat{Q}_\theta\right]\{q(\theta, \bar{p}_\theta), \theta + \alpha\}\, \mathrm{d}\theta \\ &- \frac{\partial H}{\partial p_\phi}(\gamma(\bar{p}_\theta)) \int_{-\infty}^{\infty} \hat{Q}_\theta\{q(\theta, \bar{p}_\theta), \theta + \alpha\}\, \mathrm{d}\theta. \end{aligned} \tag{5.5}$$

Note that the formulation is identical to (3.2) in nature. The integrand is evaluated along an unperturbed homoclinic motion $q(\theta, \bar{p}_\theta)$ which is based at the saddle point at $\bar{p}_\theta$ and which is parametrized by θ. Note that since $\dot{\theta}$ is single-signed, θ is monotonic if not taken to be mod(2π), and hence is asymptotic to $\pm\infty$ at the ends of the homoclinic motions.

Further details require specific expressions for the perturbations and are not considered here. In general, $M_\theta(\alpha)$ will have behavior similar to $M(\alpha)$ and it is expected that chaotic motions will exist for open sets of parameter values.

In fact, if one considers $\dot{\theta}$ (or, equivalently, p_θ) to be nominally large with small deviations, due to variations in ϕ and the conservation of angular momentum, then

$$\theta = \Omega t + \varepsilon\psi \quad \text{and} \quad \dot{\theta} = \Omega + \varepsilon\dot{\psi},$$

and θ-dependent disturbances, with terms such as $\sin(\theta)$, are approximated by $\sin(\Omega t) + \mathcal{O}(\varepsilon)$. Since these disturbances are of $\mathcal{O}(\varepsilon)$ themselves, the differences between the θ and the t formulations are pushed out to $\mathcal{O}(\varepsilon^2)$. Hence chaos will definitely exist in at least some cases.

6. Discussion

A simple physical system with "one and a half" degrees of freedom has been shown to exhibit at least two distinct types of chaotic motions under certain parameter conditions. These two chaos types are: (I) like that found in the planar nonrotating pendulum [5, 6, 16] and (II) similar to those which occur in Duffing's oscillator with negative linear stiffness (for example a buckled beam) [3, 4, 7]. These can even occur simultaneously and it is not improbable that chaotic "hopping" from one type to another may occur.

This system could be easily studied in a physical experiment. The validity of Melnikov's method in predicting steady-state chaos (strange attractors) could be checked against simulations and experiments as has been done by Moon and his co-workers [5, 7]. One might expect to see the following scenario as the parameters are varied: first, the existence of two (or possibly more) periodic steady-state motions, each of these undergoes a sequence of bifurcations resulting in two separate strange attractors (one each of Duffing and pendulum types) and finally, a crises [17] occurs in which these two attractors collide resulting in a single strange attractor. This final attractor would retain many features of both of its predecessors while permitting the chaotic hopping between them as described above. Simulation studies have verified the existence of chaotic dynamics in a speed controlled whirling pendulum [18]. In fact, pendulum-type, Duffing-type and "combination-type" strange attractors have been observed for that system.

An important feature of the system considered here is that the dynamics of the pendulum are allowed to couple back into the apparatus through which it is being driven. This is often unavoidable in an experiment and it has been shown that chaotic motions can generally persist in such a situation.

Comparing the results of the general and limiting cases (sections 3 and 4, respectively) indicates that, while chaotic motions do exist in the speed controlled case, the dynamics of the torque-controlled case are more varied. This is due primarily to the fact that the trajectories in the phase space can "escape" to large amplitudes, thus providing the possibility for sustained rotational motions and facilitating the potential "hopping" between the two types of chaos.

References

[1] S. Wiggins and P. Holmes, Homoclinic orbits in slowly varying oscillators, SIAM J. Math. Anal. 18 (1987) 612–629, and errata to appear.
[2] S. Wiggins and S.W. Shaw, Chaos and three dimensional horseshoes in slowly varying oscillators, ASME J. Appl. Mech., to appear.
[3] P.J. Holmes, A nonlinear oscillator with a strange attractor, Phil. Trans. Roy. Soc. A292 (1979) 419–448.
[4] S.W. Shaw and R.H. Rand, The transition to chaos in a simple mechanical system, preprint.
[5] F.C. Moon, J. Cusumano and P.J. Holmes, Évidence for homoclinic orbits as a precursor to chaos in a magnetic pendulum, Physica D 24 (1987) 383.
[6] F.M.A. Salam and S. Sastry, Dynamics of the forced Josephson junction circuit: The regions of chaos, IEEE Trans. on Circuits and Systems CAS-32, No. 8 (1985) 784–796.
[7] F.C. Moon and P.J. Holmes, A magnetoelastic strange attractor, J. Sound Vibr. 65 (1979) 285–296.
[8] G.B. Airy, On the regulator of the clock-work for effecting uniform movement of equatoreals, Memoirs of the Royal Astronomical Society 11 (1840) 249–267.
[9] J. Guckenheimer and P. Holmes, Nonlinear Oscillations, Dynamical Systems and Bifurcations of Vector Fields, Appl. Math. Sci. 42 (Springer, Berlin, 1983).
[10] A. Nayfeh and D. Mook, Nonlinear Oscillations (Wiley, New York, 1982).
[11] S. Wiggins and S.W. Shaw, Chaos and three dimensional horseshoes in perturbations of integrable two degrees of freedom Hamiltonian systems, unpublished notes.
[12] A.F. D'Souza and V.K. Garg, Advanced Dynamics: Modeling and Analysis (Prentice–Hall, London, 1984).

[13] S.W. Shaw and S. Wiggins, Chaotic motions of a torsional vibration absorber, ASME J. Appl. Mech., to appear.
[14] N. Fenichel, Persistence and smoothness of invariant manifolds for flows, Indiana Univ. Math. J. 21 (1971) 193–225.
[15] M. Hirsch, C.C. Pugh and M. Shub, Invariant Manifolds, Springer Lecture Notes in Mathematics, vol. 583 (Springer, Berlin, 1977).
[16] S.N. Chow and S.W. Shaw, Bifurcations of subharmonics, J. Diff. Eqs. 65 (1986) 304–320.
[17] C. Grebogi, E. Ott and J.A. Yorke, Crises, sudden changes in chaotic attractors and transient chaos, Physica D 7 (1983) 181–200.
[18] C.M. Krousgrill and A.K. Bajaj, Complex nonlinear dynamics of a rotating system, Develop. Mech. 14b (1987) 832–838.